International Journal of Research
Available at https://edupediapublications.org/journals
p-ISSN: 2348-6848
e-ISSN: 2348-795X
Volume 03 Issue 10
June 2016

Y and La Doping Effect on $Mg_{0.04}Zn_{0.96}O$ Nanopowders for Sensor Application

Basheer Kadhim Hasan
Master of Science in Physics
Department of Physics, University College of Science
Osmania University

J. Siva Kumar
Professor, Department of Physics
University College of Science, Osmania University

ABSTRACT

In this study we report the yttrium and lanthanum doping effect on $Mg_{0.04}Zn_{0.96}O$ powders prepared by wet chemical sol-gel route. The structural phase of the prepared powders is identified by X-Ray diffraction and is found that all the powders are in Hexagonal single phase without impurity peak. The microstructure and elemental analysis is done using scanning electron microscopy (SEM) equipped with energy dispersive spectra (EDS). The bonds formed in the all compounds are determined by Fourier Transform Infra Red spectroscopy technique. The structural properties obtained using UV-Visible spectroscopy technique. The doping effect is clearly observed in each technique that is used in this present work. The effect of yttrium and lanthanum doping effect on $Mg_{0.04}Zn_{0.96}O$ structure and its optical properties are explained based on the doping of rare earths in general.

International Journal of Research
Available at https://edupediapublications.org/journals
p-ISSN: 2348-6848
e-ISSN: 2348-795X
Volume 03 Issue 10
June 2016

Keywords: energy dispersive spectra (EDS), lanthanum, $Mg_{0.04}Zn_{0.96}O$, scanning electron microscopy (SEM), yttrium

Introduction

Nanoparticles are particles between 1 and 100 nanometers in size. In nanotechnology, a particle is defined as a small object that behaves as a whole unit with respect to its transport and properties. Particles are further classified according to diameter.[1] Ultrafine particles are the same as nanoparticles and between 1 and 100 nanometers in size, fine particles are sized between 100 and 2,500 nanometers, and coarse particles cover a range between 2,500 and 10,000 nanometers. Nanoparticle research is currently an area of intense scientific interest due to a wide variety of potential applications in biomedical, optical and electronic fields.[2][3][4][5] The National Nanotechnology Initiative has led to generous public funding for nanoparticle research in the United States.

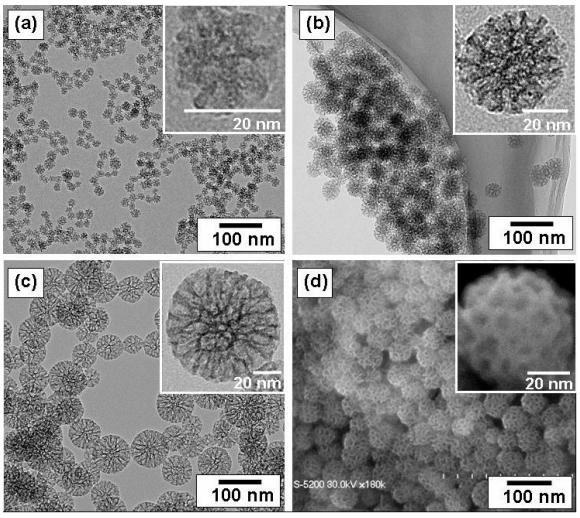

Fig. 1: TEM (a, b, and c) images of prepared mesoporous silica nanoparticles with mean outer diameter: (a) 20nm, (b) 45nm, and (c) 80nm. SEM (d) image corresponding to (b). The insets are a high magnification of mesoporous silica particle.

Properties of Nanomaterials

Nanoparticles are of great scientific interest as they are, in effect, a bridge between bulk materials and atomic or molecular structures. A bulk material should have constant physical properties regardless

of its size, but at the nano-scale size-dependent properties are often observed. Thus, the properties of materials change as their size approaches the nanoscale and as the percentage of atoms at the surface of a material becomes significant. For bulk materials larger than one micrometer (or micron), the percentage of atoms at the surface is insignificant in relation to the number of atoms in the bulk of the material. *The interesting and sometimes unexpected properties of nanoparticles are therefore largely due to the large surface area of the material, which dominates the contributions made by the small bulk of the material*.

Fig. 2: Silicon nanopowder

Nanoparticles often possess unexpected optical properties as they are small enough to confine their electrons and produce quantum effects.[4] For example, gold nanoparticles appear deep-red to black in solution. Nanoparticles of yellow gold and grey silicon are red in color. Gold nanoparticles melt at much lower temperatures (~300 °C for 2.5 nm size) than the gold slabs (1064 °C);.[31] Absorption of solar radiation is much higher in materials composed of nanoparticles than it is in thin films of continuous sheets of material. In both solar PV and solar thermal applications, controlling the size, shape, and material of the particles, it is possible to control solar absorption.

Fig. 3: 1 kg of particles of 1 mm3 has the same surface area as 1 mg of particles of 1 nm3

Other size-dependent property changes include quantum confinement in semiconductor particles, surface plasmon resonance[4] in some metal particles and superparamagnetism in magnetic materials. What would appear ironic is that the changes in physical properties are not always desirable. Ferromagnetic materials smaller than 10 nm can switch their magnetisation direction using room temperature thermal energy, thus making them unsuitable for memory storage. Suspensions of nanoparticles are possible since the interaction of the particle surface with the solvent is strong enough to overcome density differences, which otherwise usually result in a material either sinking or floating in a liquid.

The high surface area to volume ratio of nanoparticles provides a tremendous driving force for diffusion, especially at elevated temperatures. Sintering can take place at lower temperatures, over shorter time scales than for larger particles. In theory, this does not affect the density of the final product, though flow difficulties and the tendency of nanoparticles to agglomerate complicates matters. Moreover, nanoparticles have been found to impart some extra properties to various day to day products. For example, the presence of titanium dioxide nanoparticles imparts what we call the self-cleaning effect, and, the size being nano-range, the particles cannot be observed. Zinc oxide particles have been found to have superior UV blocking

properties compared to its bulk substitute. This is one of the reasons why it is often used in the preparation of sunscreen lotions, is completely photostable and toxic. Clay nanoparticles when incorporated into polymer matrices increase reinforcement, leading to stronger plastics, verifiable by a higher glass transition temperature and other mechanical property tests. These nanoparticles are hard, and impart their properties to the polymer (plastic). Nanoparticles have also been attached to textile fibers in order to create smart and functional clothing. Metal, dielectric, and semiconductor nanoparticles have been formed, as well as hybrid structures (e.g., core–shell nanoparticles). Nanoparticles made of semiconducting material may also be labeled quantum dots if they are small enough (typically sub 10 nm) that quantization of electronic energy levels occurs. Such nanoscale particles are used in biomedical applications as drug carriers or imaging agents.

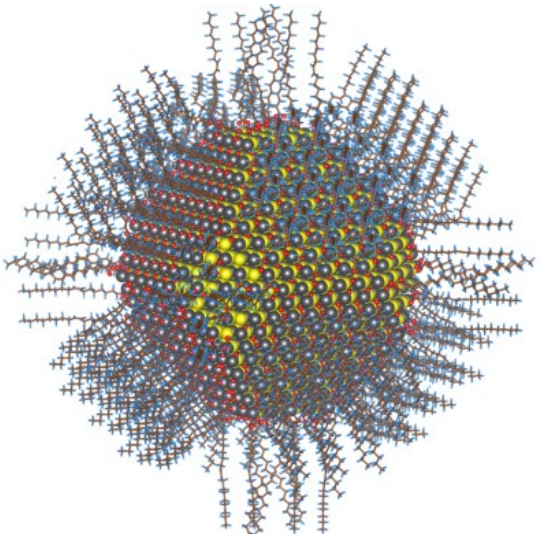

Fig.4: Semiconductor nanoparticle (quantum dot) of lead sulfide with complete passivation by oleic acid, oleyl and hydroxyl (size ~5nm)

Semi-solid and soft nanoparticles have been manufactured. A prototype nanoparticle of semi-solid nature is the liposome. Various types of liposome nanoparticles are currently used clinically as delivery systems for anticancer drugs and vaccines. Nanoparticles with one half hydrophilic and the other half hydrophobic

are termed Janus particles and are particularly effective for stabilizing emulsions. They can self-assemble at water/oil interfaces and act as solid surfactants.

SYNTHESIS METHODS

There are the several methods to prepare the nanoparticles, there are

a) Co-precipitation method

b) Hydro thermal method

c) Solvothermal method.

d) Sol- Gel method

a) Co precipitation method:

Chemical precipitation is widely used in industry and research to synthesize nanometer sized oxide powders. The process starts from dissolving salts, which contain metal ions, in a liquid medium. The solution is then mixed with a solution of dissolved precipitating agent, such as oxalic acid or ammonium hydroxide, in order to precipitate the metal oxalates or hydroxides. The final crystalline oxide is then obtained by firing the precipitates at a higher temperature. A significant problem which has to be to overcome in chemical precipitation is the agglomeration of the particles in the solution. Thus, dispersants are often added in the reaction process to provide repulsive (electrostatic or steric) interactions between the particles to prevent them from adhering to each other. To eliminate subsequent neck formation and aggregation in the calcinations and firing steps, organic solvents such as ethanol may be added in the final washing step to replace water adsorbed on the powder surface. The advantages of the precipitation method include technical simplicity, low manufacturing cost, high reproducibility and fine particle size. Disadvantages are the difficulty to control

the final chemical composition of the products and up scaling issues. Also, the repeated washing and steps make precipitation a time-consuming method.

b) Hydrothermal method:

Hydrothermal processing is one of the promising processes in materials science and engineering. The definition of hydrothermal synthesis involves H_2O as catalyst and occasionally as component of solid phases in the synthesis at elevated temperatures and pressure (>few atmosphere). The hydrothermal process is one of (>100the promising methods for preparing fine ceramic powders). The term hydrothermally usually refers to any heterogeneous reaction in the presence of aqueous solvents mineralizes under high pressure and temperature conditions to dissolve and recrystallize (recover) materials that are relatively insoluble under ordinary conditions. The powders synthesized by the hydrothermal method are well crystallized and easily dispersible in an aqueous medium. The hydrothermal process is also a good method to solve environmental and economic problems, because of its closed system and energy efficiency. This technique involves the synthesis of the materials at greatly reduced temperatures. For hydrothermal experiments the requirements for starting materials are

- ✓ accurately known composition
- ✓ as homogeneous as possible
- ✓ as pure as possible
- ✓ as fine as possible.

Nitrates or acetates in stoichiometric amounts are dissolved in deionized water. The required pH is adjusted and solution sealed in a non-corrosive vessel called autoclave. The 00°C for varying periods under auto generated pressures, the

container is then cooled to room temperature. Centrifuging temperature is maintained in between 100-200°C, then separates the solid and solution phases and the solids are washed free of dissolved salts. The main advantage of this method is that the calcinations of compounds at higher salts. The main advantage of this method is that the calcinations of compounds at higher temperatures can be avoided and higher surface areas can be obtained.

c) Solvothermal method:

Solvothermal synthesis is a method of producing chemical compounds. It is very similar to the hydrothermal route, the only difference being that the precursor solution is usually not aqueous. Thus Solvothermal synthesis allows for the precise control over the size, shape distribution, and crystallinity of metal oxide nanoparticles or Nano structures. These characteristics can be altered by changing certain experimental parameters, including reaction temperature, reaction time, solvent type, surfactant type, and precursor type. Solvothermal synthesis has been used in laboratory to make nanostructured titanium dioxide, graphene, carbon and other materials. The high photo catalytic capacity of titanium dioxide leads to the degradation of organic and biological molecules into smaller and less harmful compounds. Because of their small size, titanium dioxide nanostructures also provide increased surface area at which photo catalytic reactions may occur, increases their activity. This photo catalytic activity may be applied to air purification, self-sterilization, water purification and molecular hydrogen production.

d) Sol-Gel method:

The sol-gel method was developed in the 1960s mainly due to the need of new synthesis methods in the nuclear industry.

A sol is a stable dispersion of colloidal particles or polymers in a solvent. The particles may be amorphous or crystalline. An aerosol is particles in a gas phase while a sol is particles in a liquid.

A gel consists of a three dimensional continuous network, which encloses a liquid phase, in a colloidal gel, the network is built from agglomeration of colloidal particles. In a polymer gel the particles have a polymeric sub-structure made by aggregates of sub-colloidal particles. Typical precursors are metal alkoxides and metal chlorides, which undergo hydrolysis (Hydrolysis is a chemical reaction or process in which a chemical compound is broken down by reaction with water) and poly-condensation reactions (A chemical reaction in which two or more molecules combine upon the separation of water or some other simple substance) to form a colloid, a system composed of solid particles (size ranging from 1 nm to 1 µm) dispersed in a solvent. The sol evolves then towards the formation of an inorganic network containing a liquid phase (gel). Formation of a metal oxide involves connecting the metal centers with Oxo (M-O-M) or hydroxide (M-OH-M) bridges, therefore generating metal-Oxo or metalhydroxo polymers in solution. The drying process serves to remove the liquid phase from the gel thus forming a porous material, and then a thermal treatment (firing) may be performed in order to favor further polycondensation and enhance mechanical properties. The precursor sol can be either deposited on a substrate to form a film (e.g. by dipcoating or spin-coating), cast into a suitable container with the desired shape. (E.g. to obtain a monolithic

ceramics, glasses, fibers, membranes, aero gels), or used to synthesize powders (e.g. microspheres, Nano spheres).

The sol-gel process usually consists of 4 steps:

(1) The desired colloidal particles once dispersed in a liquid to form a sol.

(2) The deposition of sol solution produces the coatings on the substrates by spraying, dipping or spinning.

(3) The particles in sol are polymerized through the removal of the stabilizing components and produce a gel in a state of a continuous network.

(4) The final heat treatments pyrolysis the remaining organic or inorganic components and form an amorphous or crystalline coating.

The sol-gel approach is interesting in that it is a cheap and low-temperature technique that allows for the fine control on the product's chemical composition. As even small quantities of do paints, such as organic dyes and rare earth metals, can be introduced in the sol and end up in the final product finely dispersed.

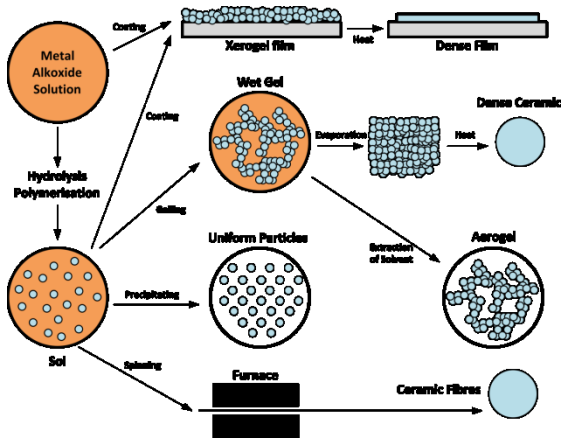

Fig 5: Schematic Overview showing two synthesis examples by the sol–gel method.

SYNTHESIS PROCEDURE

Instruments used

Magnetic stirrer, magnetic stirrer with hot plate, Glass beakers, Spatula, Digital Balance, watch Glasses, Butter Paper, Crucibles with lid, Bunsen Burner, droppers, pH paper, etc.

Synthesis of $Mg_{0.04}Zn_{0.98}O$ nanoparticles

Chemicals

Zinc nitrate, Magnesium nitrate, Citric acid, Ammonia solution, Ethylene glycol, Double distilled water, etc.

Calculations

To prepare 5 grams of Metal Oxide (MO) compound; $Mg_{0.04}Zn_{0.96}O$ is taken as an example,

Total Molecular Weight of Compound (TMWC)

= 0.04(Molecular Weight of Magnesium) + 0.96(Molecular Weight of Zinc) +1(Molecular Weight of Oxygen).

= 0.04(24.305) +0.96(65.38) +1(15.999).

= 79.736 gr/mol

- Weight of $Mg(NO_3)_2$ = $\frac{5*ratio\ of\ Mg\ in\ Compound*m.w.of\ Mg(NO_3)_2}{TMWC}$ = $\frac{5*0.04*256.41}{79.736}$ = 0.6431 gr
- Weight of $Zn(NO_3)_2$ = $\frac{5*ratio\ of\ Zn\ in\ Compound*m.w.of\ Zn(NO_3)_2}{TMWC}$ = $\frac{5*0.96*297.47}{79.736}$ = 17.9072 gr
- Weight of Citric Acid = ratio * total mole numbers of Metal ions *m.w. of citric acid
- Mole no of Mg ions = $\frac{weight\ of\ Mg(NO_3)_2\ (which\ is\ calculated\ above)}{m.w.of\ Mg(NO_3)_2}$ = $\frac{0.6431}{256.41} = 2.5082 \times 10^{-3}$

- Mole no of Zn ions = $\frac{weight\ of\ Zn(NO_3)_2\ (which\ is\ calculated\ above)}{m.w.of\ \ Cd(NO_3)_2} = \frac{17.907}{297.47} = 60.198339 \times 10^{-3}$
- Total mole numbers of Metal ions = $2.5082 \times 10^{-3} + 60.198339 \times 10^{-3} = 62.70657 \times 10^{-3}$
- Weight of Citric Acid = 1.2* 0.06270657*210.14 = 15.8125 gr.

Procedure to prepare $Mg_{0.04}Zn_{0.96}O$ nanoparticles

- Washed the Beaker, watch glass, magnetic bead, dropper and spatulas for several times before the weighing and dissolving the chemicals using acetone and deionized water.
- Weighed the precursor nitrate chemicals according the calculations in watch glass using digital balance with 0.001 precision.
- 17.907 gms of Zinc nitrate, 0.643 gms of Magnesium nitrate salts (A.R. grade chemicals) were dissolved in 500ml capacity beaker with 100ml double distilled water.
- Inserted a 1 inch magnetic bead into the beaker and stirred for homogeneous mixing using magnetic stirrer for 30 mins.
- 15.812 gms of citric acid salt was added to nitrate solution slowly with continuous stirring. This stirring process was continued for 1hr.
- Initially checked the pH value of the mixture solution using pH testing (litmus) paper.
- Then adequate ammonia solution was added to the solution drop by drop using dropper with long teat.
- After reaching the pH value 6.5–7, adding of ammonia solution was stopped and measured the quantity

of the final solution. Started heating approximately at 100 °C using magnetic stirrer with hot plate.

- After reaching 1/3rd of the initial quantity of neutralized solution, 2ml of ethylene glycol was added. And stirred for 30 min for homogeneous mixing.
- Magnetic bead was extracted from the beaker and again started heating process approximately 250 °C to obtain gel and to be burned into ash like powder.
- These ashes like powders were taken into 50 ml capacity of crucibles and burned using Bunsen burner for 30 mins.
- Then the final powder was ground for 30 min to get fine powder. The final powder samples were used to characterize and to study the further studies.

Synthesis of $Mg_{0.04}Zn_{0.98}O$:RE nanoparticles

Calculations are done using above mentioned manner and the procedure also same for the lanthanum and yttrium doped $Mg_{0.04}Zn_{0.98}O$ semiconductor compounds.

Process to prepare $Mg_{0.04}Zn_{0.96}O$:RE nanoparticles

First precursor materials like Zinc nitrate, Magnesium nitrate and rare earth nitrate (A.R. grade chemicals) were weighed according to stoichiometric ratio and dissolved in 100ml double distilled water. Citric acid solution was added to the metal nitrates solution as a chelating agent. The mixture solution was maintained at room temperature under vigorous stirring for 60 min. Liquid ammonia solution was used to neutralize the pH (6.5–7) of the solution and heated up to 80°C till a transparent and homogeneous gel was obtained. Ethylene

glycol (EG) was added to the gel. Off-white powders formed after burning were ZnCdO:RE nanoparticles.

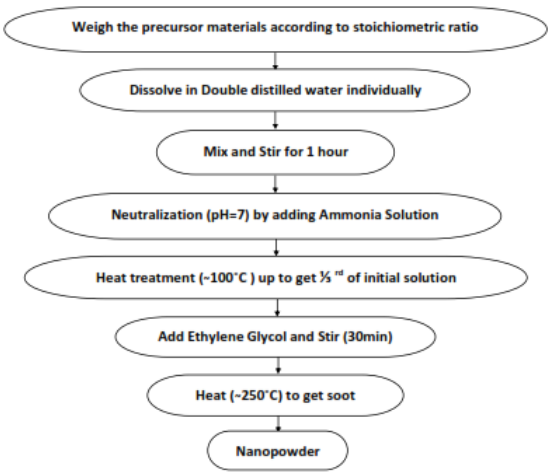

Figure 6: Flow chart for sol-gel synthesis process

RESULTS:

In this project, the following samples were prepared.

S.No.	Sample formula	Sample code
1	$Zn_{0.96}Mg_{0.04}O$	M4
2	$Zn_{0.94}Mg_{0.04}O:Y_{0.02}$	MY42
3	$Zn_{0.92}Mg_{0.04}O:Y_{0.04}$	MY44
4	$Zn_{0.94}Mg_{0.04}O:La_{0.02}$	ML42
5	$Zn_{0.92}Mg_{0.04}O:La_{0.04}$	ML44

The XRD patterns of the prepared powders were recorded on a Panalytical X'pert powder X-Ray diffractometer with CuKα radiation (λ= 1.5405Å) in the angular range of 20˚–80˚. The morphological investigation and elemental analysis of nanoparticles were obtained by a ZEISS EVO-18 Scanning Electron Microscope equipped with EDS. The stretching and bending vibration modes of the bonds formed in the compound was determined by Fourier transform infrared (FTIR) Spectro meter model SHIMADZU 8400S in the wave number range 4000-400 cm^{-1} with KBr pellets. The optical properties of nanoparticles were examined with a PG Instruments T90+ UV–Vis double beam spectrophotometer.

XRD Analysis:-

All the prepared powders were characterized by powder X-ray diffraction (XRD) with Phillips, diffractometer (Germany make) using (40 kV, 30mA) CuK-α radiation (λ= 1.5406 Å). XRD patterns were obtained in the range of 10.0100 to 79.9900 by step scanning mode with the step size of 0.0200°. Fig. 4.1 shows the XRD patterns of $Zn_{0.96}Mg_{0.04}O$, $Zn_{0.94}Mg_{0.04}O:Y_{0.02}$, $Zn_{0.92}Mg_{0.04}O:Y_{0.04}$, $Zn_{0.94}Mg_{0.04}O:La_{0.02}$ and $Zn_{0.94}Mg_{0.04}O:La_{0.04}$ samples prepared by sol-gel method The XRD data analysis shows that all the five samples are single-phase of ZnO without any other secondary phase such as MgO.

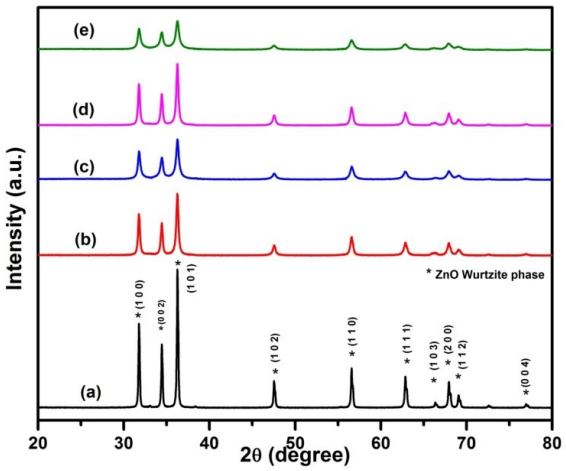

Figure 7: XRD pattern of (a) $Zn_{0.96}Mg_{0.04}O$, (b) $Zn_{0.94}Mg_{0.04}O:Y_{0.02}$, (c) $Zn_{0.92}Mg_{0.04}O:Y_{0.04}$, (d) $Zn_{0.94}Mg_{0.04}O:La_{0.02}$ and (e) $Zn_{0.92}Mg_{0.04}O:La_{0.04}$ powder samples.

The preferential orientation of all the samples has been found to be along (1 0 1) plane. Other peaks were obtained along (1 0 0), (0 0 2), (1 0 2), (1 1 0), (1 0 3), (2 0 0), (1 1 2), and (0 0 4). The analysis revealed that all the powders are of polycrystalline in nature having a hexagonal wurtzite type crystal structure according to the JCPDS files (PDF # 891397) and no peaks that correspond to either cadmium, zinc or their

complex oxides could be detected. This suggests that the samples do not have any phase segregation. The crystalline size of the films was calculated by using Debye Scherer formula, Crystallite size $(D) = \frac{0.9\,\lambda}{\beta\, Cos\theta}$. Where, λ is the wavelength of the X-Ray Source, β is the full width at half maximum (FWHM) in radians, θ is the Diffraction angle i.e., Bragg's angle. The calculated crystallite sizes are found to 35, 28, 23, 19 and 20 nm for samples M4, MY42, MY44, ML42 and ML44 respectively.

Compositional analysis (EDS):

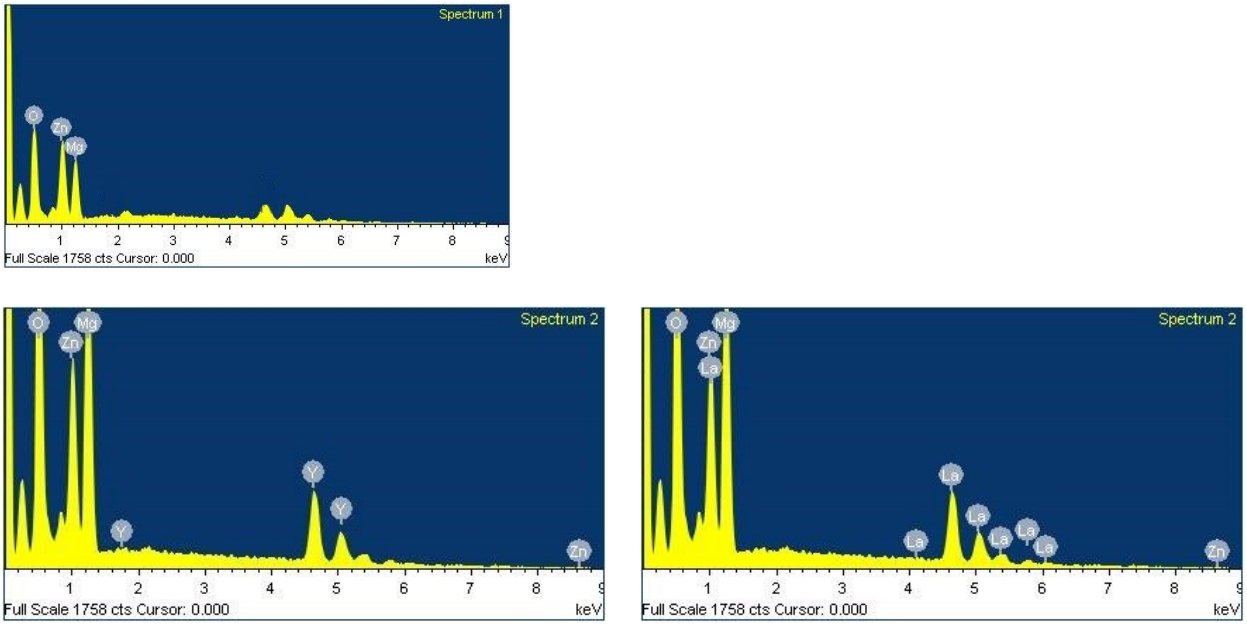

Figure 8: EDS Spectra of $Zn_{0.96}Mg_{0.04}O$ (Top), $Zn_{0.94}Mg_{0.04}O{:}Y_{0.02}$ (Left), $Zn_{0.92}Mg_{0.04}O{:}La_{0.04}$ (Right).

Compositional analysis was performed by the EDS to further determine the doping of rare earths in host compound. The EDS analysis confirmed the presence of Zn, Mg, O and rare earth (Y, La) elements in the prepared samples. The carbon observed in the spectra may probably come from the carbon tape. The EDS spectrum taken on samples M4, MY42 and ML44. The appearance of the Y, La peaks in the EDS spectrum of samples confirms the rare earth(s) incorporation in the powders. The weight percentages of samples are presented below table.

Table 1: weight percentages of samples

Sample	Weight percentages				
	Zn	Mg	O	RE (Y/La)	Total
$Zn_{0.96}Mg_{0.04}O$	78.72	1.22	20.06	--	100.00
$Zn_{0.94}Mg_{0.04}O:Y_{0.02}$	76.63	1.21	19.95	2.22	100.00
$Zn_{0.92}Mg_{0.04}O:Y_{0.04}$	74.56	1.20	19.83	4.41	100.00
$Zn_{0.94}Mg_{0.04}O:La_{0.02}$	75.68	1.20	19.70	3.42	100.00
$Zn_{0.92}Mg_{0.04}O:La_{0.04}$	72.76	1.18	19.35	6.72	100.00

Microstructure analysis (SEM):

SEM is a promising technique for the topography study of samples, as it provides valuable information regarding the growth mechanism, shape and size of particles and/or grains. Fig. 4.3 shows the SEM images of prepared powders at different magnification to allow a review of the complete growth phenomenon of the samples. The growth of the samples was observed to be uniform and well covered. From SEM Fig. 4.3, it was observed that all the prepared powder samples are smooth, homogenous and densely packed with

uniform growth of material. This image shows nature of the powders and the particles are somehow spherical. The particles are look like agglomerated this indicates that the particle size was increased due to the agglomeration of particles. The SEM micrographs have taken at different magnifications i.e. 1 µm and 200 nm. One thing we can observe that the grain size of all samples are in the range of 40-70 nm.

(a)

(b)

(c)

(d)

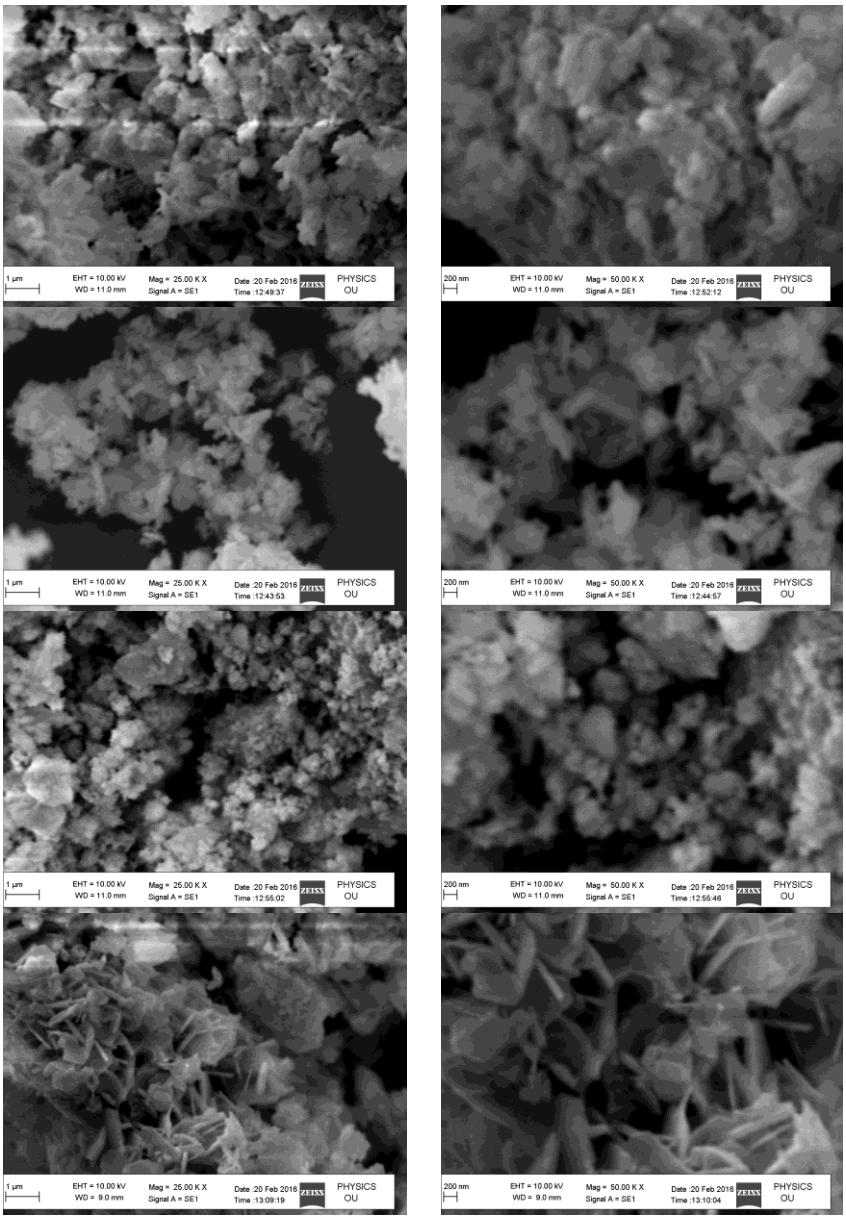

(e)

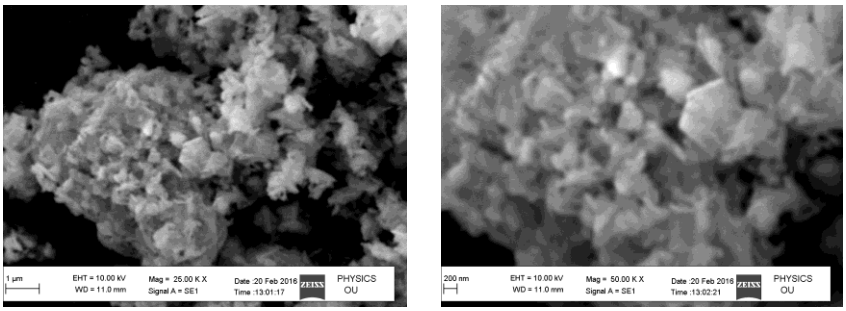

Figure 10: Microstructure of (a) $Zn_{0.96}Mg_{0.04}O$, (b) $Zn_{0.94}Mg_{0.04}O:Y_{0.02}$, (c) $Zn_{0.92}Mg_{0.04}O:Y_{0.04}$, (d) $Zn_{0.94}Mg_{0.04}O:La_{0.02}$ and (e) $Zn_{0.92}Mg_{0.04}O:La_{0.04}$ samples at 1µm and 200 nm respectively.

Fourier Transform Infra Red Spectroscopy (FTIR):-

Fourier transform infrared (FT-IR) spectroscopy was used to study the surface interactions and bonding. Frequency shifts and absorbance values were carefully observed to interpret the surface structure of ZnMgO:RE powders. The quality and composition of the prepared powders were characterized using the FTIR spectroscopy at room temperature in the range of 400–4000 cm^{-1} and shown in Fig. 4.4. The obtained spectrum show absorption bands around 504 cm^{-1} and 445 cm^{-1} which are the typical characteristic bands of the wurtzite hexagonal phase pure Zn–O and Mg–O respectively [100]. Moreover, the band at around 3433 cm^{-1} is related with the existence of hydroxyl group while the bands at 1036, 1353 and 1622 cm^{-1} are due to the presence of $–NO_3$, C–O and C=O, respectively.

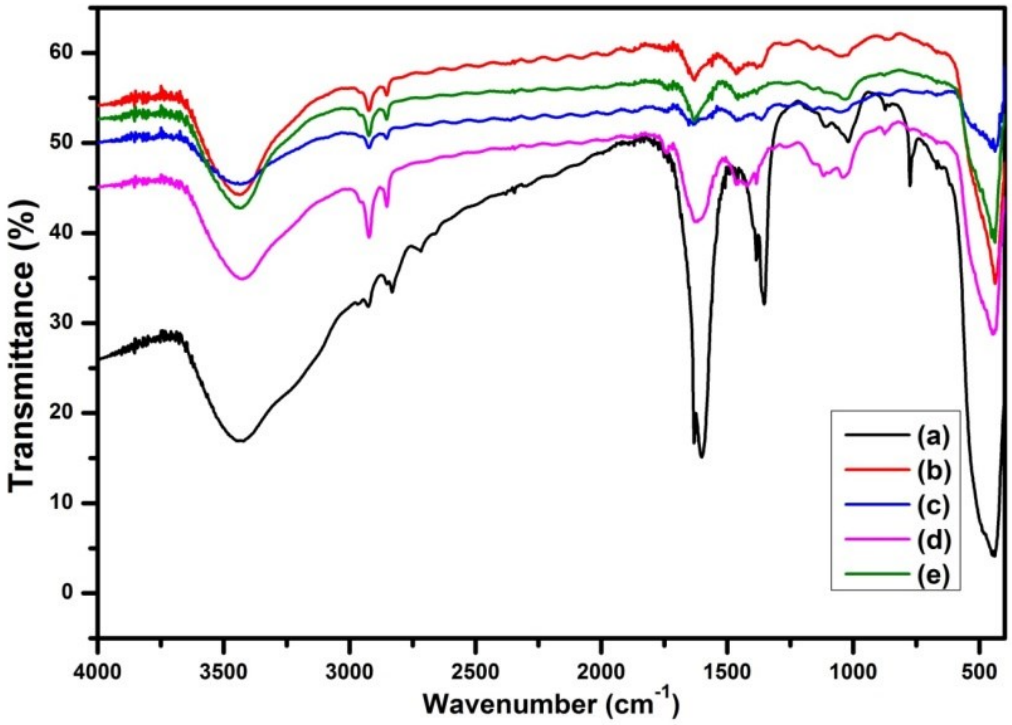

Figure 11: FTIR spectrum of (a) $Zn_{0.96}Mg_{0.04}O$, (b) $Zn_{0.94}Mg_{0.04}O:Y_{0.02}$, (c) $Zn_{0.92}Mg_{0.04}O:Y_{0.04}$, (d) $Zn_{0.94}Mg_{0.04}O:La_{0.02}$ and (e) $Zn_{0.92}Mg_{0.04}O:La_{0.04}$ nanopowder samples respectively.

UV-Visible Spectroscopy:-

In order to determine the dependence of the band gap energy on the amount of cadmium in ZnO, the position of the transmittance's first derivative peak is measured. It is expected that the transmittance's first derivative diverges at $\lambda_g=hc/E_g$, where λ_g is the position of maximum peak for the samples. The position of the peak being a measurement of the band gap energy, Eg. The first derivative of transmittance with respect to wavelength ($dT/d\lambda$), determines the band gap energy for the nanopowders [101,102]. According to our optical data analysis, the band gap energies were measured at 3.43, 3.40, 3.37, 3.37 and 3.32 eV for the $Zn_{0.96}Mg_{0.04}O$, $Zn_{0.94}Mg_{0.04}O:Y_{0.02}$, $Zn_{0.92}Mg_{0.04}O:Y_{0.04}$,

$Zn_{0.94}Mg_{0.04}O:La_{0.02}$ and $Zn_{0.92}Mg_{0.04}O:La_{0.04}$ nanopowders respectively. The observed peak position and energy gap values are tabulated in below table, which clearly shows the rare earths concentration effect on size and band gap of prepared samples.

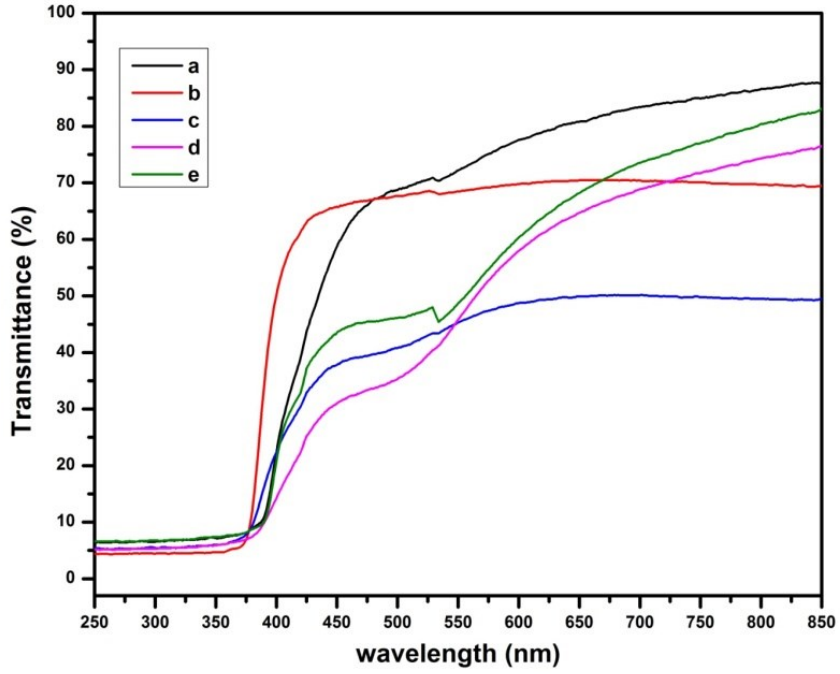

Figure 12: Optical Transmittance spectra of prepared (a) $Zn_{0.96}Mg_{0.04}O$, (b) $Zn_{0.94}Mg_{0.04}O:Y_{0.02}$, (c) $Zn_{0.92}Mg_{0.04}O:Y_{0.04}$, (d) $Zn_{0.94}Mg_{0.04}O:La_{0.02}$ and (e) $Zn_{0.92}Mg_{0.04}O:La_{0.04}$ nanopowder samples.

Sample	dT/dλ Peak position (nm)	Eg (eV)
$Zn_{0.96}Mg_{0.02}O:Y_{0.02}$	364	3.40
$Zn_{0.94}Mg_{0.02}O:Y_{0.04}$	368	3.37
$Zn_{0.96}Mg_{0.02}O:La_{0.02}$	368	3.37
$Zn_{0.94}Mg_{0.02}O:La_{0.04}$	373	3.32

Conclusions

A series of compound semiconductors $Zn_{0.98}Mg_{0.02}O$, $Zn_{0.96}Mg_{0.02}O:Y_{0.02}$, $Zn_{0.96}Mg_{0.02}O:Y_{0.04}$, $Zn_{0.96}Mg_{0.02}O:La_{0.02}$ and $Zn_{0.96}Mg_{0.02}O:La_{0.04}$ is prepared by sol-gel method. All the prepared samples were characterized by XRD, SEM, EDS, FTIR and UV-Vis techniques. XRD results show that the particles are formed in hexagonal ZnO single phase. The crystallite size found to be varied from 19 to 35 nm randomly. SEM micrographs show that all the particles are spherical in nature. EDS results reveal all the elements are present in all samples according to their composition. FTIR analysis given the information about the stretching and bending vibration band formed in the samples. Optical studies are presented using transmittance and absorbance spectra. And the optical band also tuned from 3.43 to 3.32 eV.

REFERENCES:

[1]. Module 3: Characteristics of Particles – Particle Size Categories. epa.gov

[2]. *Taylor, Robert; Coulombe, Sylvain; Otanicar, Todd; Phelan, Patrick; Gunawan, Andrey; Lv, Wei; Rosengarten, Gary; Prasher, Ravi; Tyagi, Himanshu (2013). "Small particles, big impacts: A review of the diverse applications of nanofluids". Journal of Applied Physics* ***113****: 011301. Bibcode: 2013 JAP...113a1301T. doi:10.1063/1.4754271.*

[3]. *Taylor, Robert A; Otanicar, Todd; Rosengarten, Gary (2012). "Nanofluid-based optical filter optimization for PV/T systems". Light: Science & Applications* ***1*** *(10): e34. doi:10.1038/lsa.2012.34.*

[4]. *Hewakuruppu, Y. L.; Dombrovsky, L. A.; Chen, C.; Timchenko, V.; Jiang, X.; Baek, S.; Taylor, R. A. (2013). "Plasmonic "pump–probe" method to study semi-transparent nanofluids". Applied Optics* ***52*** *(24): 6041–6050. doi:10.1364/AO.52.006041. PMID 24085009.*

[5]. *Taylor, Robert A.; Otanicar, Todd P.; Herukerrupu, Yasitha; Bremond, Fabienne; Rosengarten, Gary; Hawkes, Evatt R.; Jiang, Xuchuan; Coulombe, Sylvain (2013). "Feasibility of nanofluid-based optical filters". Applied Optics* ***52*** *(7): 1413–22. doi:10.1364/AO.52.001413. PMID 23458793.*

[6]. *Vert, M.; Doi, Y.; Hellwich, K. H.; Hess, M.; Hodge, P.; Kubisa, P.; Rinaudo, M.; Schué, F. O. (2012). "Terminology for biorelated polymers and applications (IUPAC Recommendations 2012)". Pure and Applied Chemistry* ***84*** *(2). doi:10.1351/PAC-REC-10-12-04.*

[7]. *MacNaught, Alan D. and Wilkinson, Andrew R., ed. (1997). Compendium of Chemical Terminology: IUPAC Recommendations (2nd ed.). Blackwell Science. ISBN 0865426848.*

[8]. *Alemán, J.; Chadwick, A. V.; He, J.; Hess, M.; Horie, K.; Jones, R. G.; Kratochvíl, P.; Meisel, I.; Mita, I.; Moad, G.; Penczek, S.; Stepto, R. F. T. (2007). "Definitions of terms relating to the structure and processing of sols, gels, networks, and inorganic-organic hybrid materials (IUPAC Recommendations 2007)". Pure*

and Applied Chemistry ***79*** *(10): 1801. doi:10.1351/pac200779101801.*

[9]. *Vert, Michel; Doi, Yoshiharu; Hellwich, Karl-Heinz; Hess, Michael; Hodge, Philip; Kubisa, Przemyslaw; Rinaudo, Marguerite; Schué, François (2012). "Terminology for biorelated polymers and applications (IUPAC Recommendations 2012)" (PDF). Pure and Applied Chemistry* ***84*** *(2): 377–410. doi:10.1351/PAC-REC-10-12-04.*

[10]. *Granqvist, C.; Buhrman, R.; Wyns, J.; Sievers, A. (1976). "Far-Infrared Absorption in Ultrafine Al Particles". Physical Review Letters* ***37*** *(10): 625–629. Bibcode:1976PhRvL..37..625G. doi:10.1103/PhysRevLett.37.625.*

[11]. *Hayashi, C.; Uyeda, R and Tasaki, A. (1997). Ultra-fine particles: exploratory science and technology (1997 Translation of the Japan report of the related ERATO Project 1981–86). Noyes Publications.*

[12]. *Kiss, L. B.; Söderlund, J.; Niklasson, G. A.; Granqvist, C. G. (1999). "New approach to the origin of lognormal size distributions of nanoparticles". Nanotechnology* ***10****: 25–28. doi:10.1088/0957-4484/10/1/006.*